Published in final edited form as:
Biomaterials. 2009 August ; 30(23-24): 3834–3846. doi:10.1016/j.biomaterials.2009.04.022.

Thin-film enhanced nerve guidance channels for peripheral nerve repair

Isaac P. Clements[1], **Young-tae Kim**[1,2], **Arthur W. English**[3], **Xi Lu**[1,4], **Andy Chung**[1], and **Ravi V. Bellamkonda**[1,*]

[1]Neurological Biomaterials and Cancer Therapeutics, Wallace H. Coulter Department of Biomedical Engineering, Georgia Institute of Technology/Emory University, Atlanta, GA 30332

[3]Department of Cell Biology, Emory University, Atlanta, GA

Abstract

It has been demonstrated that nerve guidance channels containing stacked thin-films of aligned poly (acrylonitrile-methacrylate) fibers support peripheral nerve regeneration across critical sized nerve gaps, without the aid of exogenous cells or proteins. Here, we explore the ability of tubular channels mininally supplemented with aligned nanofiber-based thin-films to promote endogenous nerve repair. We describe a technique for fabricating guidance channels in which individual thin-films are fixed into place within the lumen of a polysulfone tube. Because each thin-film is <10μm thick, this technique allows fine control over the positioning of aligned scaffolding substrate. We evaluated nerve regeneration through a 1-film guidance channel - containing a single continuous thin-film of aligned fibers - in comparison to a 3-film channel that provided two additional thin-film tracks. Thirty rats were implanted with one of the two channel types, and regeneration across a 14 mm tibial nerve gap was evaluated after 6 weeks and 13 weeks, using a range of morphological and functional measures. Both the 1-film and the 3-film channels supported regeneration across the nerve gap resulting in functional muscular reinnervation. Each channel type characteristically influenced the morphology of the regeneration cable. Interestingly, the 1-film channels supported enhanced regeneration compared to the 3-film channels in terms of regenerated axon profile counts and measures of nerve conduction velocity. These results suggest that minimal levels of appropriately positioned topographical cues significantly enhance guidance channel function by modulating endogenous repair mechanisms, resulting in effective bridging of critically sized peripheral nerve gaps.

1. INTRODUCTION

Peripheral nerves are capable of limited regeneration after injury, but regeneration across extended nerve gaps must be surgically facilitated. When the nerve stumps cannot be directly coapted without producing tension, the gap must instead be bridged - most commonly with autografted segments of nerve. Autograft bridging is limited, however, by the lack of availability of donor nerves, and drawbacks include the need for a secondary surgery and the

*Corresponding author: Ravi V. Bellamkonda. GCC Distinguished Scholar and Professor of Biomedical Engineering Suite 3108, 313 Ferst Dr., Wallace H Coulter Department of Biomedical Engineering, Georgia Institute of Technology/Emory University, Atlanta GA 30332-0535, ravi@gatech.edu, Tel: 404-385- 5038, Fax: 404-385-5044.
[2]Currently at Department of Bioengineering, University of Texas at Arlington, TX
[4]Currently at Department of Biomedical Engineering, Washington University in St. Louis, St. Louis, MO

loss of donor site function. Furthermore, the functional outcomes of autografting fall short of ideal, partly due to mismatch in dimension and modality between the injured and donor nerves [1,2].

Due to these limitations, engineered guidance channels have been explored as an alternative to autografts for the repair of nerve injury. The most common example of a synthetic guidance channel is a saline filled polymer channel, used to bridge the two nerve stumps. The channel isolates the gap between the nerve stumps, thereby facilitating a well-documented wound-healing type process of endogenous nerve repair [3]. Briefly, plasma derived precursors first coalesce into an oriented fibrin matrix that physically bridges the nerve gap. Non-neuronal cell types including fibroblasts and Schwann cells migrate from the nerve stumps along this acellular matrix, where they multiply and differentiate, enriching and remodeling the matrix [4,5]. Regenerating axons advance in close association with the proximally derived Schwann cells through the regeneration matrix, crossing over the nerve gap and re-entering the distal stump. Continued nerve growth and migration follows along this developing matrix, and a regenerated nerve cable is gradually formed and matured through a continued series of complex neural-glial-matrix interactions [5].

While this sequence of endogenous repair can be modulated by altering the guidance channel's physical and chemical properties, such as its material composition, permeability, or texture [6], regeneration through empty channels is limited beyond a critical gap length of 10mm for rat sciatic nerve gaps [7].

The introduction of scaffolding within the lumen of a guidance channel can also increase the channel's ability to bridge nerve gaps. For instance, materials with oriented topography are able to stimulate cellular alignment and effect topographic guidance [8-11], and have shown promise as scaffolding substrates. Classes of aligned scaffolding materials include patterned polymers, natural or synthetic microfilaments [12-14], and oriented gels and matrices composed of extracellular matrix (ECM) components [15-18] or polysaccharides [19].

Significantly, electrospun meshes of aligned sub-micron scale polymer fibers have also been demonstrated as effective scaffolding substrates with unique properties, such as high surface area-to-volume ratio, mechanical strength, and a compactly aligned topography [20-22]. As an example, our lab has previously developed guidance channels containing stacked electrospun polyacrlonitrile-methacrylate (PAN-MA) thin-films and demonstrated their ability to promote Schwann cell migration and nerve regeneration across critical sized nerve gaps without the aid of any exogenous ECM or trophic proteins [23].

Here, in a new design, we explore the concept of an enhanced nerve guidance channel, containing one or three aligned thin-films within the channel lumen. The organizing principle of this design is to modulate the regenerative wound-healing sequence to enable bridging of long gaps, while minimally obstructing the cross-sectional area available to the regenerating nerve. Briefly, the edges of electrospun thin-films are attached within the inner walls of the guidance channel, fixing the thin-films into place through the channel lumen. This arrangement enables fine control over the location of the thin-films within the lumen and furthermore prevents the thin-films from shifting over time. With a thickness of ~ 7μm, each thin-film sheet occupies only ~0.6% of the guidance channel's open cross-sectional area, yet provides a continuous track of densely aligned topographic cues, anchored through the length of the channel.

Using a 14mm tibial nerve gap model in rats, the regenerative potential of 1-film guidance channels, containing a single aligned thin-film, was compared to that of a 3-film design, in order to explore the design space of minimal enhancement to empty nerve guidance channels.

Using a combination of morphological and functional measures, nerve regeneration was evaluated at 6 and 13 weeks.

2. MATERIALS AND METHODS

2.1. Design of aligned fiber-based thin-film channels

2.1.1. Fabrication of aligned fiber thin-films—Films consisting of aligned poly (acrylontrile-co-methylacrylate, random copolymer, 4 mole percent methylacrylate) (PAN-MA) fibers were created through an electrospinning process as in our previous studies [23]. Briefly, a 15% (w/v) PAN-MA solution was prepared by dissolving PAN-MA into the organic solvent N, N-Dimethyl Formamide (DMF, Acros Organics) at 60°C. This solution was loaded into a metered syringe and dispensed for 15 minutes at a constant flow-rate of 1ml/hr through a 19 gauge needle across a voltage field of 15-18kV. The ejected polymer fibers were collected 10 cm away on a 3.8 cm diameter metal drum, rotating at approximately 2500 rpm to produce aligned fiber thin-films, which were baked for 4 hours at 60°C to remove any residual DMF. Finally, 2.2 × 14mm sheets of aligned thin-films were manually cut with a razor blade and separated from the collected polymer mass with fine forceps for use in channel construction.

2.1.2. Construction of thin-film enhanced nerve guidance channels—Polysulfone nerve guidance channels (Koch Membrane Systems) were modified to create enhanced nerve guides with aligned thin-films incorporated in their lumens. The semipermeable polysulfone tubing (inner diameter: 1.6 mm, outer diameter: 2.2 mm, molecular weight cutoff: 50kDa) was first cut into tubes of 17 mm length. These tubes were next sectioned lengthwise into 4 longitudinal sections, using a custom machined aluminum template. Under a fabrication microscope, the thin-film enhanced channels were then fabricated as part of a multistep process (Fig. 1), with each layer secured into place with a medical grade UV light curing adhesive (1187-M-SV01, Dymax). In the 1-film case, a single thin-film was secured longitudinally through the length of the tube. In the 3-film case, two additional films were fixed through the tube, distributed from each other in a “Z” formation (Fig. 1). This formation was chosen as opposed to a formation of three parallel thin-films because its construction was less complex, requiring that the polysulfone tube be split into four pieces rather than six. Notably, the 1-film guidance channels could have been constructed more simply by splitting the polysulfone tubes longitudinally into two pieces rather than four, but we fabricated the two channel types in an identical manner to minimize any structural variability. Significantly, due to the negligible thickness of each thin-film, there is minimal difference between the two designs in the percentage of luminal cross-sectional area occupied by scaffolding.

The channels were sterilized by overnight incubation under UV light followed by immersion in 70% ethanol for 30 minutes. This process was immediately followed by two 20 minute washes in sterilized deionized water and a final wash in sterilized phosphate buffered saline (PBS). The channels were then stored in sterile PBS until the implantation surgery.

2.2. *In vivo* implantation of enhanced nerve guidance channels

Enhanced guidance channel implantations to bridge 14 mm gaps in the tibial branch of the sciatic nerve were performed on anesthetized Fischer 344 rats (250-300g), as described in [23]. Briefly, the rats were anesthetized with inhaled isoflurane gas, and the surgical site was shaved and sterilized. Marcaine (0.25% w/v, Hospira, Inc.) was next administered subcutaneously for post-surgical pain relief (0.3 ml/animal). A skin incision was then made along the femoral axis, and the underlying thigh muscles were delineated with a blunt probe to expose the sciatic nerve. After the nerves were freed from overlying connective tissue, microscissors were used to transect the tibial nerve branch, slightly distal to the common peroneal - tibial bifurcation, and the nerve stumps were pulled 1.5 mm into each end of a

guidance channel and fixed into place with a single 10-0 nylon suture (Ethilon) to create a 14 mm gap. The muscles were then reapposed with 4-0 vicryl sutures (Ethicon Inc.) and the skin incision was clamped shut with wound clips (Braintree Scientific, Inc.). After the surgery, the rats were placed under a warm light, allowed to recover from anesthesia, and then housed separately with access to food and water *ad libitum* in a colony room maintained at constant temperature (19-22°C) and humidity (40-50%) on a 12:12 h light/dark cycle. To prevent toe chewing, a bitter solution (Grannick's Bitter Apple Co.) was applied twice a day to the affected foot. When further action was required, treatment with a mixture of New Skin (MedTech) and Metronidazole (ICN Biomedical Research Products) as described in [24] was administered and found to be effective. Animals were maintained in facilities approved by the Institutional Animal Care and Use Committee (IACUC) at the Georgia Institue of Technology and in accordance with the current United States Department of Agriculture, Department of Health and Human Services, and National Institutes of Health regulations and standards.

2.3 Evaluation of nerve regeneration

Nerve regeneration was assessed using histological and electrophysiological measures. Explanted channels were sectioned and evaluated (1) qualitatively, to examine the influence of the aligned thin-films in each channel type on the morphology of the regenerating nerve, and (2) quantitatively, to compare regeneration cable size and counts of numbers of regenerated axons. Functional recovery was assessed through electrophysiological measurements of nerve conduction velocity (NCV) and electromyographic (EMG) signals produced by the reinnervated muscles. Histological evaluation of motor endplates was also performed.

2.3.1 Experimental groups—Nerve regeneration through each channel type was evaluated at 6 weeks and 13 weeks post-implantation (Table 1). The 13 week time point (20 animals) was chosen to allow for an appreciable degree of functional recovery to take place, and electrophysiological assessments were conducted at this later time point only. Negative control cases with empty guidance channels were not performed because it was anticipated that little to no regeneration would occur through empty channels at this 14 mm gap length. These assumptions were based on prior work in our lab in which regeneration through empty channels of the same material failed in most cases, even across less challenging 10 mm gaps [25].

We note here that for the 13 week group, the process of electrophysiological testing and tissue harvest required several hours per animal, and so this phase of evaluation spanned a period of approximately ten days. As a result, the exact regeneration times were actually 12.5-14 weeks, but for simplicity this time point is elsewhere referred to in this study as the 13 week time point. To prevent bias in regeneration times between the 1-film and 3-film groups, animals from each group were tested in alternating fashion.

The six week time point groups (10 animals) were used to study the role of the thin-films in affecting regenerative processes at an earlier stage. Based on prior experience in our lab, it was determined that six weeks would be long enough to allow for an appreciable degree of axonal regeneration through the full length of the guidance channels, but short enough that the regeneration cable across the gap would still be at an immature state. Regeneration in the six week groups was examined using histological techniques.

2.3.2 Electrophysiological assessment of nerve regeneration—In order to assess functional recovery in the 13 week groups, electrophysiological testing was performed. Each animal was deeply anesthetized with a mixture of ketamine (65mg/kg), xylazine (7.5mg/kg), and acepromazine (0.5mg/kg), and a catheter was sutured into the intraperitoneal (IP) space to allow continued dosage during the evaluation. The site of nerve injury was exposed as during the initial surgery, and the cavity was kept moistened with mineral oil warmed to 37°C. Through

the procedure, the animals were kept warm with an infrared light, and their breathing rates and reflex responses to toe pinch stimuli were closely monitored.

2.3.3. Nerve conduction velocity—A portion of the sciatic nerve, approximately 15 mm proximal to the proximal end of the channel, was freed from the surrounding tissue, as was a portion of the distal tibial nerve branch, approximately 15 mm past the distal end of the channel. Stainless steel bipolar hook electrodes were fixed to both exposed portions of nerve, and the separation distance between the pair of electrodes was precisely measured. The distally positioned pair of electrodes, which was attached to a stimulator (Model S88, Grass Technologies) and stimulus isolation unit (Model SIU5B, Grass), was used to stimulate the regenerated nerve with 100μs square pulses of variable amplitude, applied at a rate of 1Hz. The evoked compound nerve action potentials (CNAPs) were recorded from the proximal pair of electrodes, amplified (G=1000), bandpass filtered (10-5000 Hz, Model 1700, A-M Systems), and digitally sampled. (25 kS/sec, Multichannel Systems DAQ card.) The recordings were averaged up to 200 times, using a trigger signal provided by the stimulator, and the latencies of the onset of the evoked CNAPs were determined off-line. The precise distances between stimulating and recording electrodes were measured and divided by the latencies to calculate the conduction velocity of the CNAPs through the regenerated nerves. Average conduction velocities through the 1-film and 3-film groups were compared using one-way ANOVA, with a p-value less than 0.05 considered statistically significant. Although the NCV does not provide a complete measure of functional recovery, this measurement is positively correlated with the size of myelinated axons and degree of myelination, and can thus be used to quantitatively assess the extent of reinnervation of the distal nerve segment.

2.3.4. EMG recordings—As an assessment of functional muscle reinnervation, bipolar patch electrodes were fixed to the surface of the denervated lateral gastrocnemius muscles (LG) and used to record evoked EMG activity. Briefly, the patch electrodes were constructed as previously described [26] by gluing two insulated, stranded, stainless steel wires through a Dacron mesh reinforced square of 0.01” thick silicone.

Hook electrodes were used to stimulate the regenerated tibial nerve with supramaximal square pulses of 300μs duration, delivered at 1Hz, and the evoked EMG signals were recorded with the patch electrodes. Recordings were amplified, filtered, and stored for off-line averaging and analysis. As a negative control, EMG activity from the tibialis anterior (TA) muscle was recorded as well, since TA is not innervated by the tibial nerve. Additionally, near the end of the procedure, the regenerated nerve was crushed distal to the stimulating hook electrode to further demonstrate that the previously recorded EMG signals from LG were indeed the result of nerve activity traveling through the regenerated nerve. Because recorded EMG signal shape and amplitude can vary significantly based on electrode placement, EMG recordings were used primarily for qualitative analysis.

2.3.5. Immunohistochemical analysis of nerve regeneration—After electrophysiological evaluation, the rats were immediately perfused intracardially with saline followed by 4% paraformaldehyde in PBS (Sigma-Aldrich). The injury site was fully exposed, and the nerve guidance channels were explanted for histological analysis. The gastrocnemius muscles from the experimental and control legs were also explanted, and all harvested tissues were post-fixed overnight in 4% paraformaldehyde. The tissues were later washed and stored for several hours in PBS and then transferred to a 30% sucrose in PBS solution for cryoprotection and incubated at 4°C for 1-2 days until saturation. Finally, the samples were embedded in O.C.T. gel (Tissue Tek) and frozen for cryosectioning (CM30505, Leica). Ten micron thick cross sections were collected at one millimeter intervals. In four channels, 18μm thick longitudinal sections were instead collected, to provide an alternative perspective of regeneration through the channels.

Sections were later reacted for immunofluorescent demonstration of markers on 1) axons (NF160, 1:500 dilution, Sigma-Aldrich); 2) Schwann cells, (S100, 1:250, Dako); 3) myelin (P0, 1:100, Chemicon Intl.); 4) macrophages (ED-1, CD-68, 1:1000, Serotec); 5) fibroblasts (vimentin, 1:500, Sigma-Aldrich, as well as S100, to allow differentiation of weak reactivity of Schwann cells by anti-vimentin antibody). Nuclei were labeled with DAPI (Invitrogen) in PBS at a concentration of 10μM. The following secondary antibodies were used: Goat anti-rabbit IgG Alexa 488/594, goat anti-mouse IgG1 Alexa 488/594, and goat anti-chick IgG (Invitrogen).

Immunohistochemistry techniques were conducted as previously described [23]. Briefly, sections were first incubated for one hour at room temperature in a blocking solution of 4% goat serum (Gibco) in PBS containing 0.5% Triton X-100 (Sigma). Sections were then incubated overnight at 4°C in a mixture of primary antibody and blocking solution, then washed and incubated once more for 1 hour at room temperature in a solution of secondary antibody, diluted 1:220 in 0.5% triton in PBS. This incubation was followed by a 10 minute incubation in DAPI solution. Finally, the sections were washed once more, dried, and cover-slipped for evaluation. Other slides were prepared for bright field microscopy using standard Masson's Trichrome staining techniques.

The cross sectional area of the regeneration cables was measured at the channel center (7 mm into the nerve gap) and at distances of 2.5 mm from each nerve stump in all 13 week channels. To perform these measurements, 4x magnified images of stained cross sections were analyzed with Image Pro software (Media Cybernetics). Within each imaged section, the cross-sectional area occupied by the regenerated tissue cable (comprised of the axonal/Schwann cell core as well the surrounding epineurial-like collagenous tissue) was selected and quantified, and means were calculated for each group.

Nerve regeneration was also quantified by counting the total number of NF-160$^+$ axonal profiles at the center of the nerve gap. To perform this analysis, a confocal microscope (LSM 510, Zeiss) was first used to image a representative subset of the regeneration cable at 40x magnification. The number of NF160$^+$ axons within this image was then quantified with Image Pro software and used to calculate a representative axonal density for each channel. Next, a composite 40x image of the entire regeneration cable cross section was obtained, using a microscope equipped with a computer controlled stage and Neurolucida software (MFB Bioscience). Image Pro software was then used to quantify the entire cross-sectional area of axonal regeneration, and this area was multiplied by the calculated axonal density to estimate the total number of axonal profiles. Accuracy of this technique was initially validated by comparing results with manual hand counts, and reproducibility/precision was demonstrated by repeating quantifications on sequential sections. One-way ANOVA was used for all statistical comparisons between the 1-film and 3-film groups, and a p-value < 0.05 was considered to be significant.

2.3.6. Evaluation of neuromuscular junctions re-innervation—Explanted gastrocnemius muscles were embedded in OCT gel in a process similar to the guidance channels and then cut with a cryostat into 25 μm thick longitudinal sections. Tissue sections were collected from the center of the muscle and reacted as previously described [23,27] for fluorescent demonstration of axons, motor endplates, and synaptic vesicles. These structures were identified using markers for neurofilament 160 (anti-NF160, Sigma-Aldrich), (2) synaptic vesicles (anti-synaptic vesicle protein 2 (SV2), Developmental Studies Hybridoma Bank), and acetylcholine receptors (tetramethlyrhodamine conjugated α-bungarotoxin, Sigma-Aldrich). Co-localization of markers for axons and motor endplates indicates morphological innervation of the neuromuscular synapses. The additional co-localization of synaptic vesicle markers is

suggestive of functional regeneration. Healthy contralateral gastrocnemius muscles taken from the control limb were evaluated as positive controls.

3. RESULTS

3.1. Surgical outcomes

All 30 rats survived the guidance channel implantation surgery without complication, and most animals exhibited only minimal autotomy as a result of nerve transection. One animal from the 1-film channel, 13 week group excessively chewed the foot on the operated side and was euthanized at two weeks post-surgery. A second animal from the 3-film, 13 week group was electively euthanized as well to allow for a comparative example of early regeneration after two weeks through each channel type. The channels explanted from these two animals were cryosectioned longitudinally for histology. All other animals remained healthy and were sacrificed at their scheduled endpoints. At the time of explantation, all guidance channels were found to be structurally intact with the tibial nerve still firmly secured on each end. The guidance channels were encased in a characteristic thin envelope of fibrotic tissue, but the visible inflammatory response to the implanted channels was otherwise minimal.

3.2. Histological assessment of nerve regeneration

3.2.1. General observations—Explanted channels were sectioned and processed for histological analysis. Substantial regeneration of $NF160^+$ axons was observed through the full lengths of both types of guidance channels at both the 6 week and 13 week time points. The aligned PAN-MA thin-films were visible in the guidance channel cross-sections and were observed to have remained intact and fixed into place within the channel interiors. The thin-films were measured to have a relatively uniform thickness of approximately 7 μm.

The placement of the aligned thin-films influenced the positioning and morphology of the regenerated nerve structure, as observed in channel cross-sections. The regeneration cables in the 1-film channels were centered around the single thin-film, and consisted of a centralized core of axons and co-localized Schwann cells that was surrounded by epineurial-like tissue arranged into aligned bands (Fig. 2A,B). The regeneration cables in the 3-film channels were larger, but contained a fragmented core of axons/Schwann cells, with subsets of this core asymmetrically dispersed around and between the multiple thin-films (Fig. 2C,D).

A minimal inflammatory response to all implanted materials, including the polysulfone walls, UV curing adhesive, and PAN-MA thin-films was observed, which was consistent with the results of our previous studies [23,28]. By the 13 week time point $ED\text{-}1^+$ macrophages were present in a thin layer on the interior and exterior surfaces of the guidance channel walls, within the walls, and were sparsely distributed within the channel interiors (data not shown). Several concentric layers of $vimentin^+$ fibroblasts surrounded the outer walls of the guidance channels, and in many of the channels fibroblast in-growth occurred through cracks at the junctures where the channel walls were cut and glued during the fabrication process (Fig. 6A). Macrophage and fibroblast presence on the thin-films was minimal.

3.2.2. 1-film channels, 13 week time point—To examine the influence of the aligned thin-films on regeneration cable morphology, cross-sections were taken at one millimeter intervals through the entire length of the channel. Characteristic patterns of regeneration observed in the 1-film channel, 13 week group are shown for a representative channel in Figure 3. Near the proximal edge of the channel, the intact nerve stump contained a core of axons arranged in a circular cross-section (Fig. 3A), but at further distances into the channel, regenerating axons were grouped together into a more centralized interior core with a cross-sectional shape that was elongated to match the orientation of the single aligned thin-film (Fig.

3B-D). This elongation of the axonal core's cross-sectional shape around the thin-film reached a maximum near the channel midpoint (Fig. 3C). At farther distances past the midpoint, the axonal core gradually regained a circular cross-section as it approached the intact distal nerve stump (Fig. 3D, E).

Patterns of cellular distribution within the core of regenerated axons also varied based on distance into the 1-film channel (Fig. 3F-H). Towards the proximal end of the regeneration cable, axons were grouped into a dense and uniformly organized pattern surrounding the single thin-film (Fig. 3F and inset). Towards the channel midpoint, the axons were aggregated into dense groups (Fig. 3G and inset). At distances past the channel midpoint, the axons were dispersed from this grouped arrangement and were distributed more uniformly, though more sparsely, across a wider cross-sectional area within the channels (Fig. 3H and inset). Co-localization of axons and Schwann cells, myelination of axons, and laminin deposition around axons were visualized at 40x magnification using confocal microscopy (Fig. 3J-L).

Surrounding the axonal core, aligned bands of epineurial-like collagenous tissue formed the periphery of the regeneration cable (Fig. 2A, 3I). These tissue bands were not attached to the smooth interior walls of the guidance channels, but in some channels attached to the junctures where the channel was cut and glued during the fabrication process, giving some of the regeneration cables a rectangular cross-sectional profile (Fig. 2A, 3B-D). The distribution of cells within the regeneration cable was correlated with the locations of the collagen bands. For example, the distribution of axons into elongated groups located within the collagen bands was apparent near the periphery of the axonal core, especially towards the distal end of the regeneration cable (Fig. 3H and inset).

1-film guidance channel cross-sections were also reacted for immunofluorescent demonstration of fibroblasts (anti-vimentin antibody). Outside the regeneration cable, the densest regions of vimentin immunoreactivity were observed surrounding the outer wall of the channels and within the porous channel walls (Fig. 4). Within the regeneration cable, vimentin^{+} fibroblasts were concentrated within the collagenous periphery, and were aligned circumferentially within the collagen tissue bands, as described by others [29] (Fig. 4C). Significantly, the axonal/Schwann cell core and the surrounding fibroblast-rich bands of collagenous tissue were well segregated into distinct regions with a defined border, (Fig. 4B,C) and only a sparse distribution of vimentin^{+} fibroblasts was observed within the axonal/Schwann cell core.

3.2.3. 3-film channels, 13 week time point—Patterns of regeneration in the 3-film, 13 week channels differed characteristically from those observed in their 1-film counterparts. In 3-film channel cross-sections (Fig. 5), the regeneration cables were compartmentalized by the thin-films into four distinct zones of differing cellular organization. For example, near the proximal end of this representative channel (Fig. 5B, F), an area of densely grouped axons was visible in the zone below the bottom thin-film (marked with a "4"), while few axons were located in the zone above the topmost thin-film (marked with a "1"). The inner zones of the 3-film channels, (marked "2" and "3" in Fig. 5F), contained a more sparse and irregular distribution of axons. As in the 1-film channels, axons in all zones were aggregated into grouped formations towards the channel midpoint (Fig. 5C, G and inset), and at further distances in the channel were dispersed more sparsely in elongated distributions that correlated with the structure of the banded collagenous tissue (Fig. 5D, H and inset). Confocal microscopy was used to visualize axon / Schwann cell co-localization, myelination of axons, and laminin deposition around axons (Fig. 5J-L).

The collagen tissue bands in the 3-film channels were distinct not only on the periphery, but also within the interior regions of the regeneration cable (Fig. 2B, Fig. 5F-I). In the outer zones,

the collagen bands had a predominantly linear / circumferential alignment as in the 1-film channels, but in the inner zones (between the outer two thin-films) alignment patterns were irregular. Rather than being arranged concentrically or in parallel, the collagen bands in these interior zones were formed into a branching structure with irregular alignment patterns that were visibly constrained by the thin-films.

Vimentin$^+$ fibroblasts were again observed surrounding the outer wall of the guidance channel, within the channel walls, and within the collagenous outer periphery of the regeneration cable (Fig. 6). However, the strict segregation of fibroblasts and Schwann cells noted in the 1-film channels was disrupted in the interior of the 3-film channels (Fig. 6B,C). In this representative channel, in the outer zone below the lowest aligned thin-film, was a dense group of co-localized Schwann cells and axons, well segregated from the fibroblasts in the periphery of the regeneration cable (Fig. 6A, B). In contrast, within the inner zones, the distribution of Schwann cells / axons was sparse and irregular (Fig. 6B) and was intermingled with groups of unaligned fibroblasts (Fig. 6C).

3.2.4. Quantitative comparisons of regeneration cable size and number of regenerated axons at 13 weeks—The cross-sectional areas of all regeneration cables at the 13 week time point were quantified at three distances into the channels (Fig. 7A). The regeneration cables in the 3-film channels were found to be significantly larger at each of these distances. At the channel midpoint, for example, the regeneration cables of the 3-film channels were found to be 1.35 times larger than the regeneration cables in the 1-film channels ($p<0.05$). In neither channel type did the size of the regeneration cable vary significantly based on distance into the channel.

Axons were regenerated through the full length all 1-film and 3-film channels in the 13 week groups. Despite the fact that the 3-film channels contained larger regeneration cables, the 1-film channels contained significantly higher numbers of NF160$^+$ regenerated axons (Fig. 7B, $p<0.01$). Compared to the 3-film channels, the 1-film channels contained on average 1.63 times the number of regenerated axon profiles, as measured from the channel midpoints (4383 ± 442 NF160$^+$ axons compared to 2691 ± 338 axons).

3.2.5. Six week time point—The six week time point was used to examine regeneration cable morphology at an earlier stage of development. By six weeks, substantial axonal regeneration had occurred through the full lengths of all 1-film channels, and through all but one of the 3-film channels. In both guidance channel types, general patterns of regeneration cable morphology were similar between the 6 and 13 week time points.

For example, characteristic differences in cellular organization between the inner and outer zones of the 3-film channels were apparent in the 6 week group (Fig. 8). As at the 13 week time point, the outer zones contained a compact distribution of co-localized axons and Schwann cells, lying adjacent to aligned collagen bands containing aligned fibroblasts (Fig. 8B,C). The inner zones contained splintered groups of axons and Schwann cells that intermingled with randomly aligned fibroblasts (Fig. 8B,D).

Although the basic regeneration cable structure was in place by the 6 week time point, regeneration in both channel types was clearly less developed than at 13 weeks. For example, the areas occupied by axonal growth were comparatively smaller and less developed, especially towards the distal ends of the 6 week channels (Fig. 9A). Also, while NF160$^+$ axons were never observed apart from Schwann cells at either time point, there existed distal portions of the 6 week regeneration cables occupied by Schwann cells alone (Fig. 9B). The distribution of axons into elongated groups that followed the banded structure of the collagenous tissue was also more prominent at the six week time point (Fig. 9C). Aligned bands of collagenous tissue were

visible not only on the periphery, but also within the interior of the regeneration cables of the 1-film channels (data not shown).

3.2.6. Longitudinal sections of explanted channels—One channel of each type was sectioned longitudinally at the six week time point and also at two weeks post-surgery to give a perspective of nerve morphology along the axis of regeneration. In sections from the 3-film channel at the six week time point, patterns of longitudinal alignment differed between the zones (Fig. 10). In the top outer zone, above the outermost thin-film (marked with a dashed line), axons, co-localized Schwann cells, and overlying collagenous tissue bands were all longitudinally aligned through the channel length (Fig. 10B, above the white dashed line). Within the inner zone on the opposite side of the same thin-film, axons/Schwann cells intermingled with misaligned fibroblasts, and longitudinal alignment patterns were disrupted (Fig. 10C).

One guidance channel of each type was also sectioned longitudinally two weeks post-implantation (Fig. 11). In both guidance channel types, axons (and co-localized Schwann cells) had migrated approximately 1/3 of the way through the length of the channels (Fig. 11A-C), and Schwann cells migrating from the distal end had covered a similar distance. Fibroblasts had migrated through the entire length of both channels by the 2 week time point.

The effects of compartmentalization within the 3-film channel were evident, as some of the zones were preferentially populated with axons and non-neuronal cells as compared to others. For example, axons had regenerated asymmetrically into the topmost outer zone, perhaps influenced in this case by the off-center location of the proximal nerve stump. Migrated fibroblasts preferentially populated the lower two zones of the 3-film channel (Fig. 11D), and the cell density and degree of alignment differed within each of these adjacent zones. Highly aligned Schwann cells trailed the fibroblasts and had migrated directly on the thin-films, as well as some distance away from the films, both on top of each other and through the developing regeneration cable framework (Fig. 11E).

3.3. Electrophysiological assessment of nerve regeneration

3.3.1. Nerve Conduction Velocity (NCV)—All 13 week time point animals from the 1-film and 3-film groups underwent electrophysiological testing at their end points. Nerve conduction velocities (NCV) across the regenerated nerves were determined by evoking compound nerve action potentials and dividing inter-electrode distance by conduction latency. A significantly higher average NCV was measured in nerves regenerated through 1-film channels as compared to nerves regenerated through the 3-film channels (20.55 ± 1.5 m/s vs. 15.86 ± 1.5 m/s, $p<0.05$) (Fig. 12A).

3.3.2. EMG signal measurements—In all animals from the 13 week time point, EMG activity was elicited by upstream stimulation of the regenerated nerve and recorded from the lateral gastrocnemius muscle (LG), which is normally innervated by the tibial nerve. In all regenerated animals, LG contracted visibly in response to tibial nerve stimulation produced a clearly distinguishable EMG signal (Fig. 12B). In contrast, the tibialis anterior (TA) muscle, normally innervated by the common peroneal nerve branch, exhibited no visible contractions in response to tibial nerve stimulation and produced no measurable EMG signal. At the end of the procedure, when the regenerated tibial nerve was crushed distal to the stimulating electrode, visible contractions and measurable EMG singles from LG disappeared in all cases. Thus, we conclude that the observed muscle contractions were indeed due to reinnervation by the regenerated tibial nerve.

3.3.3. Motor endplate reinnervation—As another assessment of muscle reinnervation by the regenerated tibial nerve, gastrocnemius muscles from the 13 week groups were longitudinally sectioned and reacted for immunofluorescent demonstration of axons, motor endplates, and synaptic vesicles (Fig. 12C-E). All muscle sections contained visible motor endplates, with a percentage of these endplates co-localized with synaptic vesicles and regenerated axons. These results indicate reinnervation in all animals from the 13 week group. The presence of synaptic vesicle proteins further suggests that the observed reinnervation was functional, agreeing with the results of EMG testing.

4. DISCUSSION

A critical first step in the sequence of endogenous nerve repair across a gap is the proper formation of an aligned, regenerative fibrin matrix/cable between the nerve stumps. The fibrin matrix provides physical support to the initial influx of migrating fibroblasts and Schwann cells, and the fine topographic structure of the matrix furthermore determines the distribution and alignment of these cells [4,5]. The regenerating cells in turn form the framework of the regeneration cable, replacing the fibrin matrix with a more permanent network of ECM proteins, including collagens and laminins [5,30-34]. The initial formation of the fibrin cable thus predetermines at an early time the final morphology of the regenerating nerve [32,35].

In similar fashion, scaffolding materials presented within a guidance channel can also impact early cellular migration and alignment to influence formative stages of endogenous nerve repair mechanisms. Internal scaffolding may act by a combination of (1) bolstering the fibrin matrix, by contributing to its proper formation and maintenance, and (2) replacing the function of the matrix, by serving as an alternative aligned substrate for glial and neuronal migration [13,14]. In either case, the proper distribution of appropriately structured scaffolding material is critical in directing the ultimate migration and alignment of regenerating cells. Disorganized topographic guidance cues – provided directly by scaffolding substrate or indirectly by a malformed fibrin matrix – can disrupt regeneration [23,31,36].

With these issues in mind, we investigated how minimal amounts of precisely distributed PAN-MA thin-films, presenting topographic cues, might promote and influence regeneration cable formation and nerve regeneration, thus enhancing the function of nerve guidance channels. We bridged critical sized nerve gaps with guidance channels containing one or three aligned thin-films, and in all 18 animals evaluated at the 13 week time point, we observed axonal regeneration and functional reinnervation of muscle. Functional reinnervation was evidenced by evoked muscle twitches and EMG recordings, and was further suggested by immunohistochemical analysis of reinnervated motor end plates. While EMG signals from reinnervated LG were measurable in all animals from each group, we observed variability in EMG signal shape and amplitude based on the precise orientation of the recording electrode on the muscle. Due to this uncontrollable variability, we used EMG measurements to qualitatively detect successful regeneration but not to quantitatively assess and compare functional recovery between the two groups. In future studies, analysis of muscle force generation in response to nerve stimulation might represent a more ideal measure of functional recovery.

The ability of the thin-film enhanced guidance channels to promote nerve regeneration across critical sized gaps was significant, given the small amounts of scaffolding material used within the guidance channels. Each thin-film occupied only 0.6% of the guidance channel's open space. (Elsewhere this measurement is termed the "packing density [14]," or, conversely, the "void fraction [37].") The packing density of our 3-film, and especially our 1-film channels, was substantially lower than in other guidance channels containing internal scaffolding described in the literature [14,36-39].

While both the 1-film and 3-film guidance channels supported regeneration across the nerve gap, regeneration through the 1-film channels was superior in terms of morphological and functional measures. Although NCV values of neither experimental group was large enough in comparison to intact rat nerve to indicate complete regeneration at this 13 week time point, these measurements demonstrate a more complete stage of regeneration in the animals treated with the 1-film channels.

The sequence of regeneration through the 1-film channels was characteristically shaped by the presence of the single aligned thin-film. Two weeks after channel implantation, a cellular matrix including aligned Schwann cells and regenerating axons had bridged the nerve gap and was centralized around the thin-film. By the six week time point, the bulk of the developing regeneration cable's framework consisted of an orderly collagenous tissue structure, arranged into aligned bands that were shaped around the thin-film.

This aligned banded configuration of collagen tissue potentially shaped the sequence of development observed in the 1-film channels. By the 13 week time point, elongated groupings of axons/Schwann cells within prominent bands of aligned collagen tissue were visible only within cross-sections taken towards the less mature distal ends of the channels (Fig. 3H and inset). These observations suggest a possible sequence of nerve maturation in which bands of axons and Schwann cells growing within the aligned bands of tissue matrix gradually merge and compact to form a more uniform and consolidated core. In this scenario, the orderly compaction of the collagen bands would be made possible by their parallel aligned structure, which formed around the single aligned thin-film early in the regeneration process. The eventual structure of the nerves regenerated through the 1-film channels consisted of a consolidated axonal core, segregated from a surrounding periphery of fibroblast-rich bands of epineurial-like tissue.

These outcomes differ from earlier reports describing regeneration across shorter gaps through guidance channels that were similarly bisected, but with thicker substrate dividers of smooth or rough (but not aligned) topographies [36,40]. These reports describe the formation of two discrete regenerated nerve cables on either side of the non-aligned divider, with each cable surrounded with an epineurial-like periphery. The aligned topography of our thin-films likely played a role in causing the differences we observed, by contributing to the proper formation of the initial regeneration cable and the directed migration and alignment of regenerative cells. Another possible contributing factor was the comparatively higher permeability and molecular weight cutoff of our PAN-MA thin-films (at least as high as 70 KDa in unpublished experiments). Biochemical factors able to pass through the permeable thin-film might have influenced cells on the opposite side, helping to consolidate the nerve cables.

In contrast to the 1-film case, regeneration cables in the 3-film channels were characterized by disrupted patterns of cellular distribution and alignment, and contained a fragmented core of fewer overall axons. Because all other design features of the two guidance channel types were identical, we conclude that the differences in regeneration stemmed from the inclusion of the two additional thin-films, which likely affected endogenous regenerative processes by a combination of mechanisms.

One effect of the additional thin-films was to compartmentalize the guidance channel into four zones. Regenerating axons and cells migrating from the nerve stumps often traveled preferentially into one or more of these zones, possibly due in part to the relative location of the sutured nerve stumps (Fig. 11B). The resulting asymmetric distribution of regeneration between the zones potentially affected regeneration adversely in at least two ways. First, constraining regeneration to a subset of the guidance channel decreases the open space available for continued growth and maturation. Secondly, as we observed at the earlier six

week time point, the zones that receiving the most regeneration from the proximal end were not necessarily the same zones receiving the most regeneration from the distal end. This mismatch in symmetry is undesirable because if non-neuronal cells and axons traveling from the proximal and distal ends do not unite at the midpoint of a given zone, initial cellular bridging fails, potentially disrupting subsequent regeneration in that zone. Indeed in the 3-film 13 week case, we observed that axon populations within a given zone sometimes began high on the proximal end and then often tapered off sharply before reaching the channel midpoint - potentially due to failed initial cellular bridge formation within that zone. Although the 1-film channels were similarly divided into two zones, the observed degree of asymmetry in regeneration between these two zones was far less than in the 3-film channels. This is possibly due to the fact that, with each compartment comprising half of the channel's cross-sectional area, the possibility of regeneration from either nerve stump significantly missing either zone was reduced.

Another potential cause for disrupted regeneration through the 3-film channels was the rearranged distribution of topographical cues caused by the additional two thin-films. Of the four zones delineated by the thin-films, the two semi-circular outer zones, (labeled "1" and "4" in Fig. 5F), were bordered by the smooth wall of the guidance channel on the outer side, and by an aligned thin-film on their interior side. This arrangement of border topography is similar to each of the two zones of the 1-film channel. Indeed, the patterns of regeneration in the outer two zones of the 3-film channels were typically comparable to those in the 1-film case in terms of cellular distribution, alignment, and segregation. In contrast, the two triangular "inner" zones of the 3-film channels, (labeled "2" and "3" in Fig. 5F), were bordered on their two long sides by the aligned thin-films, with only the third, shorter border formed by the smooth channel wall. Within the inner compartments, misaligned fibroblasts intermingled with sparse distributions of poorly aligned axons and Schwann cells, and the organization of the aligned collagen bands was also disrupted. The rearranged border topography within these inner zones potentially affected regeneration by altering the initial polymerization of aligned fibrin strands [36]. An altered initial fibrin matrix would then interfere with Schwann cell and fibroblast distribution and alignment, possibly disrupting the natural sequence leading to their segregation. Additionally, the resulting irregularly branched structure of the regeneration cable's collagenous framework in the inner zones potentially interfered with normal maturation processes leading to a consolidated axonal core.

While the arrangement of three thin-films into a 'Z' formation represents one of many possible configurations for a multiple thin-film channel, results from the 3-film channels can be extended to guidance scaffold design in general. Increased amounts of scaffolding material, even with negligible change in packing density, do not necessarily translate into enhanced regeneration. Compartmentalization of the guidance channel interior and altered distributions of topographic cues are examples of factors that can impact endogenous repair processes from an early time point and significantly impact regenerative outcomes.

5. CONCLUSIONS

In this study, nerve guidance channels enhanced with aligned thin-films presented within their lumen were designed to modulate endogenous repair processes and enhance regeneration across critically sized peripheral nerve gaps. These thin-film enhanced guidance channels contained minimal internal scaffolding, and yet promoted robust levels of axonal regeneration, without the aid of any exogenous ECM or trophic factors. When comparing regeneration through guidance channels containing one or three thin-films, significantly greater regeneration was observed in the 1-film channels. Furthermore, regenerated nerve cables through the 1-film channels were structurally more akin to normal nerve in terms of patterns of cellular distribution and alignment. These results highlight the potential influence of internal scaffolding on the

endogenous repair sequence. By providing minimal, yet appropriate topographic cues, a guidance channel's ability to bridge critically sized nerve defects may be significantly enhanced.

Acknowledgments

The authors would like to acknowledge support from the following grants: NIH R01 44409, NSF GTEC EEC-9731643, NSF CBET 0651716, and NSF IGERT-0221600. We would also like to thank He Zheng and Alex Stroh for their assistance with microscopy and quantification techniques, Dr. Brani Vidakovic for his assistance with statistical methods, and Dr. Laura O'Farrell, for her assistance with animal care.

References

1. Nichols CM, Brenner MJ, Fox IK, Tung TH, Hunter DA, Rickman SR, et al. Effect of motor versus sensory nerve grafts on peripheral nerve regeneration. Experimental Neurology 2004;190(2):347–355. [PubMed: 15530874]
2. Matsuyama T, Mackay M, Midha R. Peripheral nerve repair and grafting techniques: A review. Neurologia Medico-Chirurgica 2000;40(4):187–199. [PubMed: 10853317]
3. Williams LR, Longo FM, Powell HC, Lundborg G, Varon S. Spatial-temporal progress of peripheral-nerve regeneration within a silicone chamber - parameters for a bioassay. Journal of Comparative Neurology 1983;218(4):460–470. [PubMed: 6619324]
4. Williams LR. Exogenous fibrin matrix precursors stimulate the temporal progress of nerve regeneration within a silicone chamber. Neurochemical Research 1987;12(10):851–860. [PubMed: 3683735]
5. Liu HM. The role of extracellular-matrix in peripheral-nerve regeneration - a wound chamber study. Acta Neuropathologica 1992;83(5):469–474. [PubMed: 1621504]
6. Aebischer P, Guenard V, Winn SR, Valentini RF, Galletti PM. Blind-ended semipermeable guidance channels support peripheral-nerve regeneration in the absence of a distal nerve stump. Brain Research 1988;454(12):179–187. [PubMed: 3409002]
7. Lundborg G, Dahlin LB, Danielsen N, Gelberman RH, Longo FM, Powell HC, et al. Nerve regeneration in silicone chambers - influence of gap length and of distal stump components. Experimental Neurology 1982;76(2):361–375. [PubMed: 7095058]
8. Miller C, Shanks H, Witt A, Rutkowski G, Mallapragada S. Oriented Schwann cell growth on micropatterned biodegradable polymer substrates. Biomaterials 2001;22(11):1263–1269. [PubMed: 11336298]
9. Thompson DM, Buettner HM. Neurite outgrowth is directed by Schwann cell alignment in the absence of other guidance cues. Annals of Biomedical Engineering 2006;34(4):669–676.
10. Manwaring ME, Walsh JF, Tresco PA. Contact guidance induced organization of extracellular matrix. Biomaterials 2004;25(17):3631–3638. [PubMed: 15020137]
11. Curtis A, Wilkinson C. Topographical control of cells. Biomaterials 1997;18(24):1573–1583. [PubMed: 9613804]
12. Matsumoto K, Ohnishi K, Kiyotani T, Sekine T, Ueda H, Nakamura T, et al. Peripheral nerve regeneration across an 80-mm gap bridged by a polyglycolic acid (PGA)-collagen tube filled with laminin-coated collagen fibers: a histological and electrophysiological evaluation of regenerated nerves. Brain Research 2000;868(2):315–328. [PubMed: 10854584]
13. Lundborg G, Kanje M. Bioartificial nerve grafts - A prototype. Scandinavian Journal of Plastic and Reconstructive Surgery and Hand Surgery 1996;30(2):105–110. [PubMed: 8815979]
14. Ngo TT, Waggoner PJ, Romero AA, Nelson KD, Eberhart RC, Smith GM. Poly(L-lactide) microfilaments enhance peripheral nerve regeneration across extended nerve lesions. Journal of Neuroscience Research 2003;72(2):227–238. [PubMed: 12671998]
15. Ceballos D, Navarro X, Dubey N, Wendelschafer-Crabb G, Kennedy WR, Tranquillo RT. Magnetically aligned collagen gel filling a collagen nerve guide improves peripheral nerve regeneration. Experimental Neurology 1999;158(2):290–300. [PubMed: 10415137]
16. Whitworth IH, Brown RA, Dore C, Green CJ, Terenghi G. Orientated mats of fibronectin as a conduit material for use in peripheral-nerve repair. Journal of Hand Surgery-British and European Volume 1995;20B(4):429–436.

17. Dodla MC, Bellamkonda RV. Differences between the effect of anisotropic and isotropic laminin and nerve growth factor presenting scaffolds on nerve regeneration across long peripheral nerve gaps. Biomaterials 2008;29(1):33–46. [PubMed: 17931702]

18. Stokols S, Tuszynski MH. Freeze-dried agarose scaffolds with uniaxial channels stimulate and guide linear axonal growth following spinal cord injury. Biomaterials 2006;27(3):443–451. [PubMed: 16099032]

19. Chamberlain LJ, Yannas IV, Hsu HP, Strichartz G, Spector M. Collagen-GAG substrate enhances the quality of nerve regeneration through collagen tubes up to level of autograft. Experimental Neurology 1998;154(2):315–329. [PubMed: 9878170]

20. Yang F, Murugan R, Wang S, Ramakrishna S. Electrospinning of nano/micro scale poly(L-lactic acid) aligned fibers and their potential in neural tissue engineering. Biomaterials 2005;26(15):2603–2610. [PubMed: 15585263]

21. Schnell E, Klinkhammer K, Balzer S, Brook G, Klee D, Dalton P, et al. Guidance of glial cell. migration and axonal growth on electrospun nanofibers of poly-epsilon-caprolactone and a collagen/poly-epsilon-caprolactone blend. Biomaterials 2007;28(19):3012–3025. [PubMed: 17408736]

22. Huang ZM, Zhang YZ, Kotaki M, Ramakrishna S. A review on polymer nanofibers by electrospinning and their applications in nanocomposites. Composites Science and Technology 2003;63(15):2223–2253.

23. Kim YT, Haftel VK, Kumar S, Bellamkonda RV. The role of aligned polymer fiber-based constructs in the bridging of long peripheral nerve gaps. Biomaterials 2008;29(21):3117–3127. [PubMed: 18448163]

24. Zhang YP, Onifer SM, Burke DA, Shields CB. A topical mixture for preventing, abolishing, and treating autophagia and self-mutilation in laboratory rats. Contemporary Topics in Laboratory Animal Science 2001;40(2):35–36. [PubMed: 11300686]

25. Yu XJ, Bellamkonda RV. Tissue-engineered scaffolds are effective alternatives to autografts for bridging peripheral nerve gaps. Tissue Engineering 2003;9(3):421–430. [PubMed: 12857410]

26. Loeb, GE.; Gans, C. Electromyography for Experimentalists. Chicago: The University of Chicago Press; 1986.

27. Dodla MC, Bellamkonda RV. Differences between the effect of anisotropic and isotropic laminin and nerve growth factor presenting scaffolds on nerve regeneration across long peripheral nerve gaps. Biomaterials 2008;29(1):33–46. [PubMed: 17931702]

28. Clements, IP.; Kim, YT.; Andreasen, D.; Bellamkonda, RV. A regenerative electrode scaffold for peripheral nerve interfacing. Proceedings of the 3rd International Conference IEEE Engineering in Medicine and Biology Society Conference on Neural Engineering; 2007 May 2-5; Kohala Coast, HI, USA. 2007. p. 390-393.

29. Scaravilli F. Regeneration of the perineurium across a surgically induced gap in a nerve encased in a plastic tube. Journal of Anatomy 1984;139:411–424. [PubMed: 6490525]

30. Williams LR, Powell HC, Lundborg G, Varon S. Competence of nerve-tissue as distal insert promoting nerve regeneration in a silicone chamber. Brain Research 1984;293(2):201–211. [PubMed: 6697215]

31. Aebischer P, Guenard V, Valentini RF. The morphology of regenerating peripheral-nerves is modulated by the surface microgeometry of polymeric guidance channels. Brain Research 1990;531(12):211–218. [PubMed: 2289122]

32. Williams LR, Varon S. Modification of fibrin matrix formation insitu enhances nerve regeneration in silicone chambers. Journal of Comparative Neurology 1985;231(2):209–220. [PubMed: 3968235]

33. Williams LR, Danielsen N, Muller H, Varon S. Exogenous matrix precursors promote functional nerve regeneration across a 15-mm gap within a silicone chamber in the rat. Journal of Comparative Neurology 1987;264(2):284–290. [PubMed: 3680633]

34. Scaravilli F. The influence of distal environment on peripheral-nerve regeneration across a gap. Journal of Neurocytology 1984;13(6):1027–1041. [PubMed: 6534972]

35. Zhao Q, Dahlin LB, Kanje M, Lundborg G. Repair of the transected rat sciatic-nerve - matrix formation within implanted silicone tubes. Restorative Neurology and Neuroscience 1993;5(3):197–204.

36. Guenard V, Valentini RF, Aebischer P. Influence of surface texture of polymeric sheets on peripheral-nerve regeneration in a 2-compartment guidance-system. Biomaterials 1991;12(2):259–263. [PubMed: 1878462]

37. Li JM, Shi RY. Fabrication of patterned multi-walled poly-L-lactic acid conduits for nerve regeneration. Journal of Neuroscience Methods 2007;165:257–264. [PubMed: 17644184]

38. Itoh S, Takakuda K, Ichinose S, Kikuchi M, Schinomiya K. A study of induction of nerve regeneration using bioabsorbable tubes. Journal of Reconstructive Microsurgery 2001;17(2):115–123. [PubMed: 11310749]

39. Lundborg G, Dahlin L, Dohl D, Kanje M, Terada N. A new type of “bioartificial” nerve graft for bridging extended defects in nerves. Journal of Hand Surgery-British and European Volume 1997;22B(3):299–303.

40. Danielsen N, Vahlsing HL, Manthorpe M, Varon S. A 2-compartment modification of the silicone chamber model for nerve regeneration. Experimental Neurology 1988;99(3):622–635. [PubMed: 3342845]

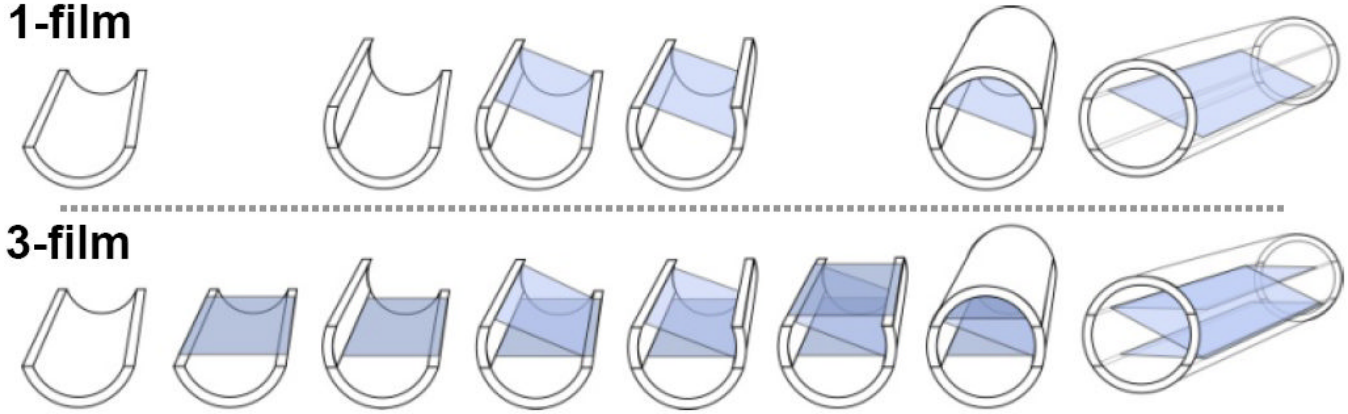

Fig. 1.

Illustration of the fabrication process for a 1-film (top row) and 3-film (bottom row) channel. Under a microscope, longitudinal sections of polysulfone tubing and strips of electrospun PAN-MA thin-films were sequentially stacked and fixed into place with UV curing adhesive. The steps used to build the two channel types were identical, except for the addition of the two extra thin-films included in the 3-film channels.

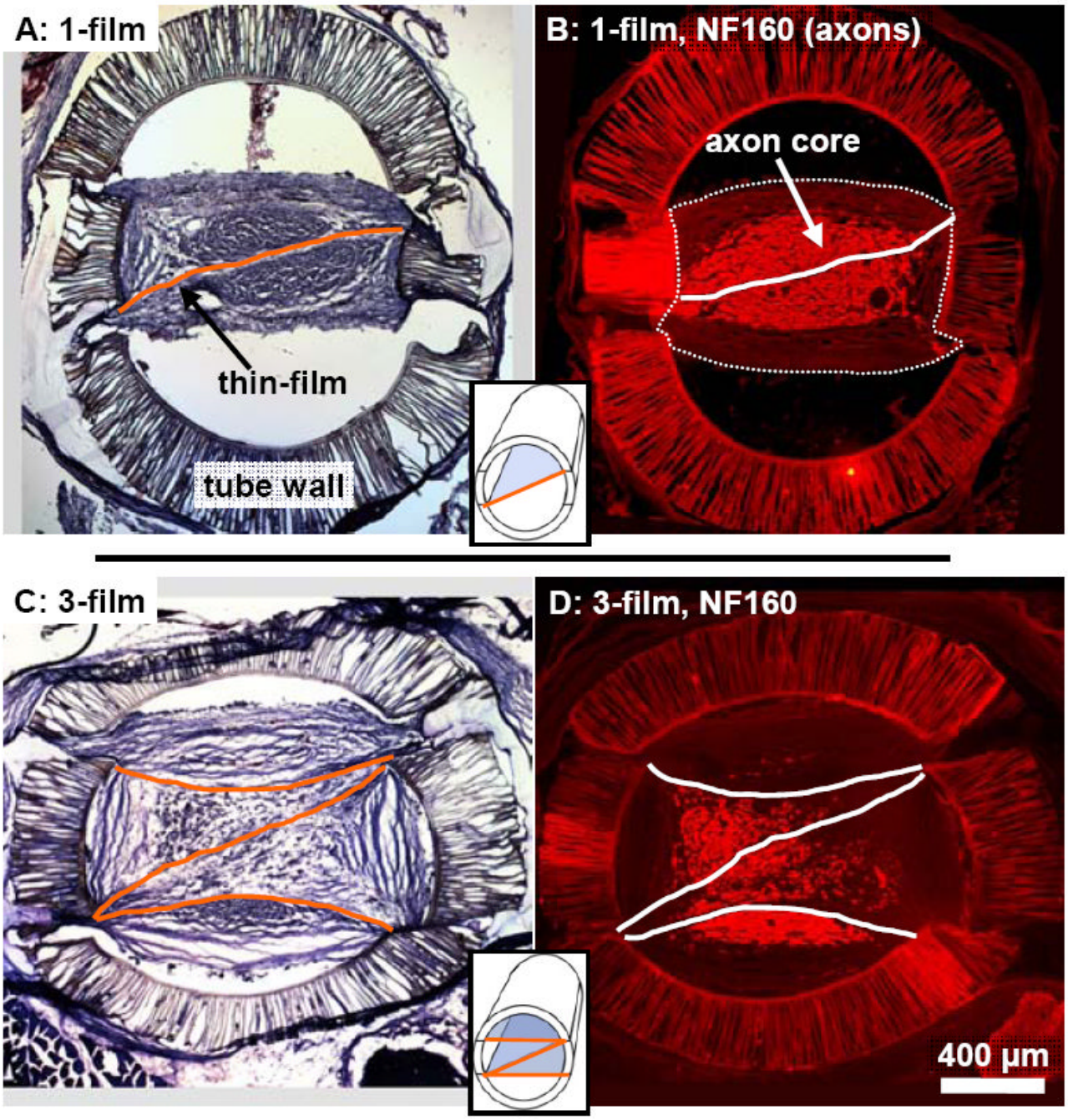

Fig. 2.

Representative cross-sections from a 1-film (A,B) and 3-film (C,D) channel at the 13 week time point. False colored lines mark the locations of the aligned thin-films. (A,C): Tissue stained cross-sections taken 3.5 mm into the nerve gap. The location and structure of the regenerated tissue cables were visibly influenced by the thin-films. (B,D): Cross-sections taken from 2.5 mm into the nerve gap, reacted with NF160 for immunofluorescent demonstration of axons. In the 1-film channels (B), regenerated axons were distributed within a consolidated core surrounding the single thin-film. This core was surrounded by aligned bands of epineurial-like tissue forming the periphery of the regeneration cable, (the outer border of which is marked

with a thin dotted line). In the 3-film channels, the axonal core was fragmented around and between the aligned thin-films.

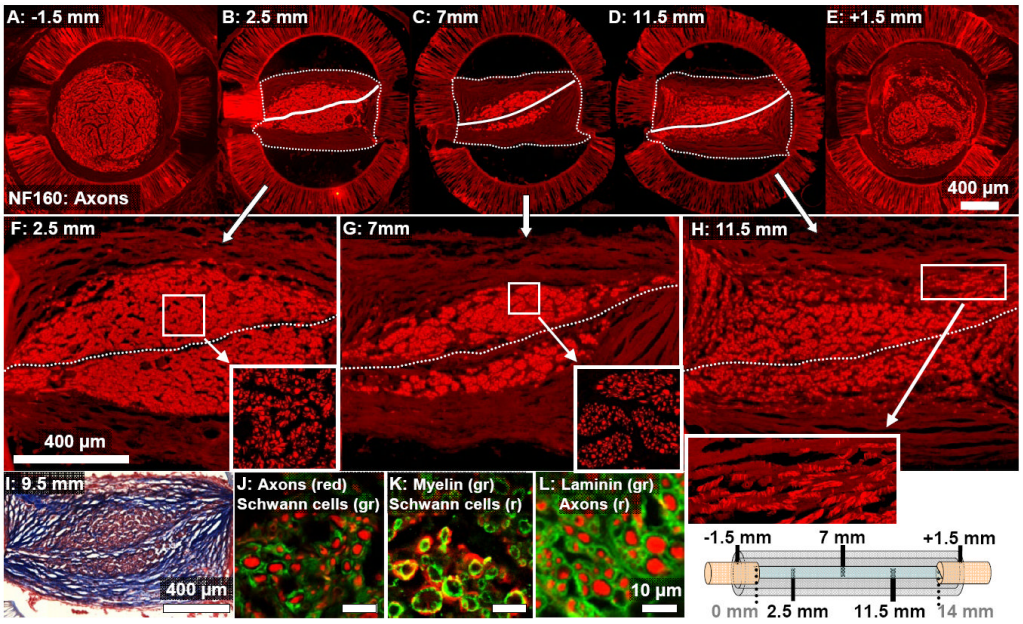

Fig. 3.

Cross-sections taken at increasing distances into a representative 1-film channel at the 13 week time point (see diagram at bottom right corner.) (A-E): The brightly fluorescent core of $NF160^{+}$ axons is consolidated around the single aligned thin-film (marked by a solid white line.) This axonal core was surrounded by bands of collagenous tissue forming the regeneration cable periphery. (These bands are more dimly visible, and their outer border is marked with a dotted line.) (F-H): Magnified images of the regeneration cables shown in (B-D). Axons towards the proximal end of the channel were densely grouped into a consolidated core (F). Near the channel midpoint, axons were aggregated into isolated groups (G). Past the midpoint, axons were dispersed across a wider area and distributed in patterns correlated with the locations of the aligned collagen tissue bands (H and inset.) (I): These collagen bands were aligned in formations oriented in parallel to the surface of the aligned thin-film (Masson's Trichrome stain). Sections were reacted for immunofluorescent demonstration of (J): axons and Schwann cells (S100), (K): Schwann cells and Myelin (P0), and (L): axons and Laminin-1.

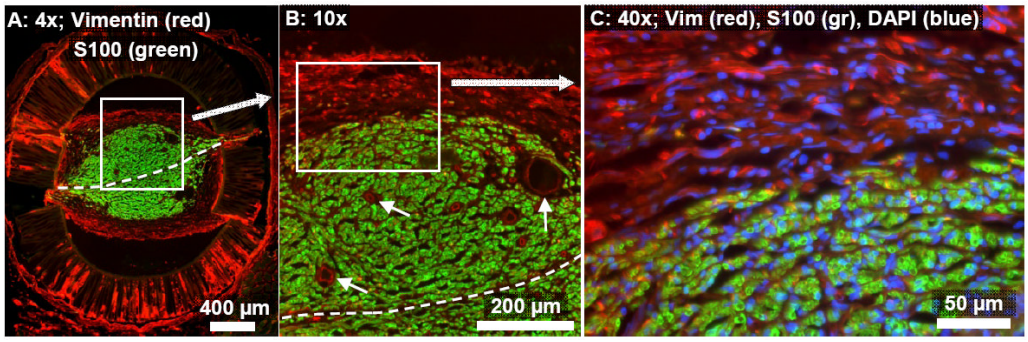

Fig. 4.

Cross-section from the same representative 1-film channel as in Fig. 3, taken 1.5 mm into the nerve gap and processed for immunofluorescent demonstration of fibroblasts (vimentin: red) and Schwann cells (S100: green). (A): Vimentin^{+} fibroblasts were visible within the bands of collagenous tissue surrounding the axonal/Schwann cell core, particularly in the outer periphery. (B): Magnified view of the boxed region in (A). The axonal core is segregated from the surrounding fibroblast-rich collagenous tissue. Several example blood vessels are marked by small arrows. (C): Magnified view of the boxed region in (B). Fibroblasts were located mainly outside of the Schwann cell / axonal core and were aligned within the epineurial-like bands of collagenous tissue.

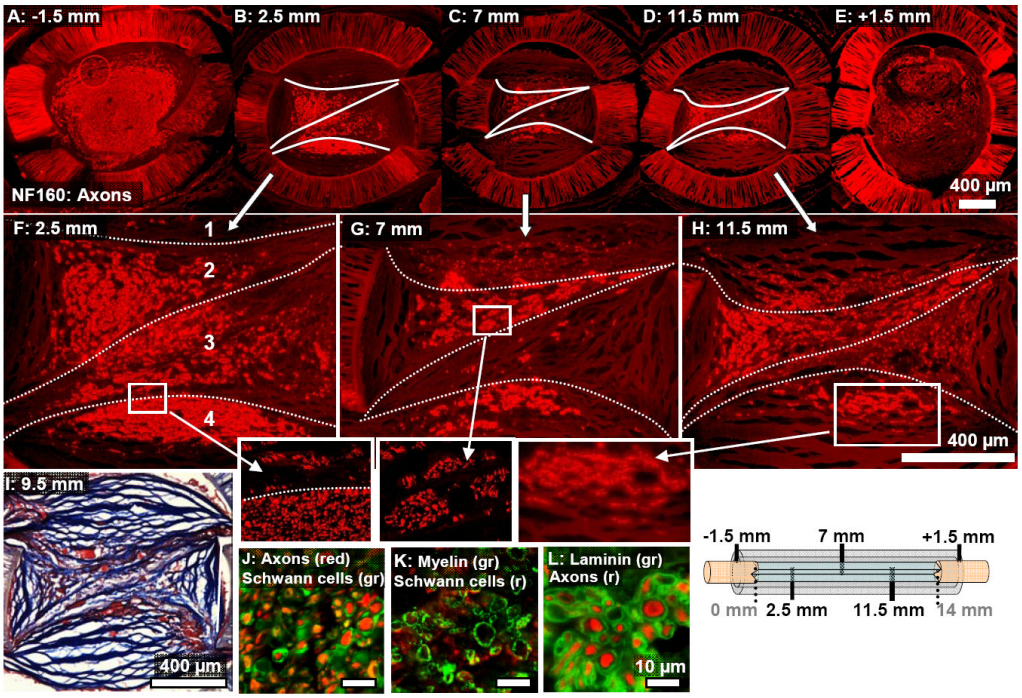

Fig. 5.

Cross-sections taken at increasing distances into a representative 3-film channel at the 13 week time point. (A-E): The axonal core (NF160) was fragmented asymmetrically around the thin-films, whose approximate location is marked with white lines. (F-H): Magnified images of (B-D). (F): The three thin-films compartmentalized the channel into four zones (labeled “1”-”4”) Axons in the lower outer zone (labeled “4”) were densely grouped, but within the interior compartments (“2” and “3”), axons were more sparsely distributed. Little regeneration was observed in the top compartment, (“1”). (G): Axons showed a tendency to aggregate in tight groups near the channel mid-point. (H and inset): Axons were more dispersed past the channel midpoint and were distributed according to the structure of the collagenous bands. (I): In the interior zones of the channel, the alignment of the collagenous banded structure was disrupted (Masson’s Trichrome stain). Sections were reacted for immunofluorescent demonstration of (J): axons and Schwann cells (S100), (K): Schwann cells and Myelin (P0), and (L): axons and Laminin-1.

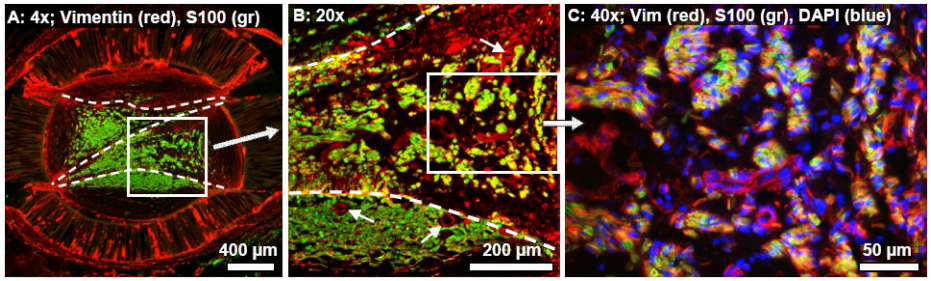

Fig. 6.

Cross-section from the same representative 1-film channel as in Fig. 5, taken 1.5 mm into the nerve gap and processed for immunofluorescent demonstration of fibroblasts (vimentin: red) and Schwann cells (S100: green). (A): Vimentin^{+} fibroblasts were visible in the outer bands of collagenous tissue. (B): Magnified view of the boxed region in (A). In the outer zone below the lower thin-film was a dense and consolidated portion of the axonal core. (Example blood vessels are indicated with small arrows). In the interior zone above this lower thin-film, the Schwann cells/axonal distribution was sparse, irregular, and intermixed with vimentin^{+} fibroblasts. (C): Magnified view of the boxed region in (B). Schwann cells and randomly aligned fibroblasts intermingled within the interior compartments of the regeneration cable.

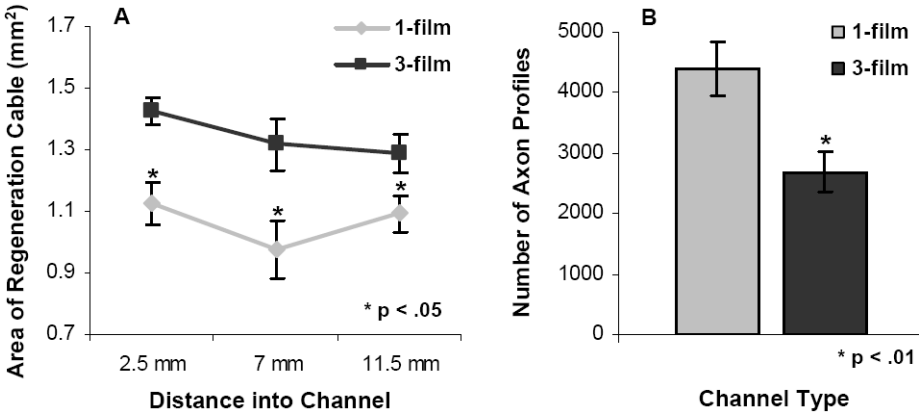

Fig. 7.

Quantitative comparison of regeneration cables in each channel type. (A): Cross-sectional areas of the regeneration cables (including the collagenous tissue periphery) were quantified at three distances into each channel. The regeneration cables in the 3-film channels were significantly larger at each distance as compared to the 1-film channels. There were no significant differences in regeneration cable sizes between the different distances into the channels. (B): Axon profiles were quantified at the midpoint of each channel at the 13 week time point. Despite containing smaller regeneration cables, the 1-film channels supported significantly higher counts of regenerating axon profiles. (Error bars represent s.e.m.)

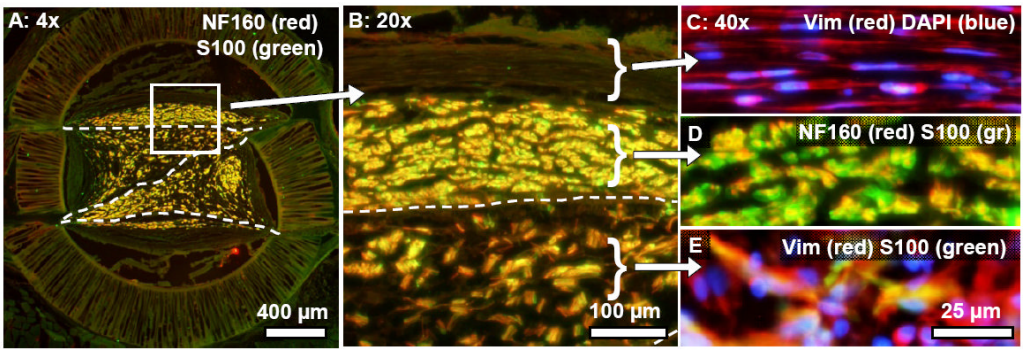

Fig. 8.

Cross-sections taken near the proximal end of a representative 3-film channel at the six week time point, illustrating similarities in regeneration cable morphology between the 6 and 13 week time points. (A): Axons (NF160: red) and Schwann cells (S100: green) were co-localized and distributed within the compartments of the 3-film channels, as in the 13 week channels. (B): Magnified view of the boxed region in (A). Patterns of cellular organization in the inner and outer zones differed characteristically. (C): Fibroblasts (vimentin: red) in the epineurial-like collagenous bands were highly aligned and well segregated from underlying groups of axons/Schwann cells (D). (E): Within the interior compartments of the 3-film channel, randomly aligned fibroblasts intermingled with Schwann cells/axons.

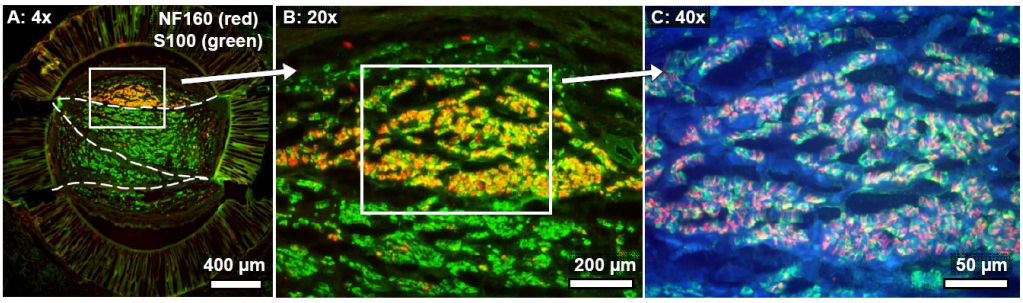

Fig. 9.

Cross-section taken near the distal end of a representative 3-film channel at the six week time point. (A): Migrated Schwann cells (S100: green) were distributed throughout the channel, but regenerated axons (NF160: red) were present mainly in the top outer zone of the channel. In the more mature regeneration cables at the 13 week time point, Schwann cells and axons were fully co-localized throughout the channel. (B): Magnified view of the boxed region in (A), showing the distribution of axons and Schwann cells. C): Further magnification of the boxed region in B). Schwann cell / axon localization within the collagenous bands was prominent. (The collagenous tissue is emphasized in blue).

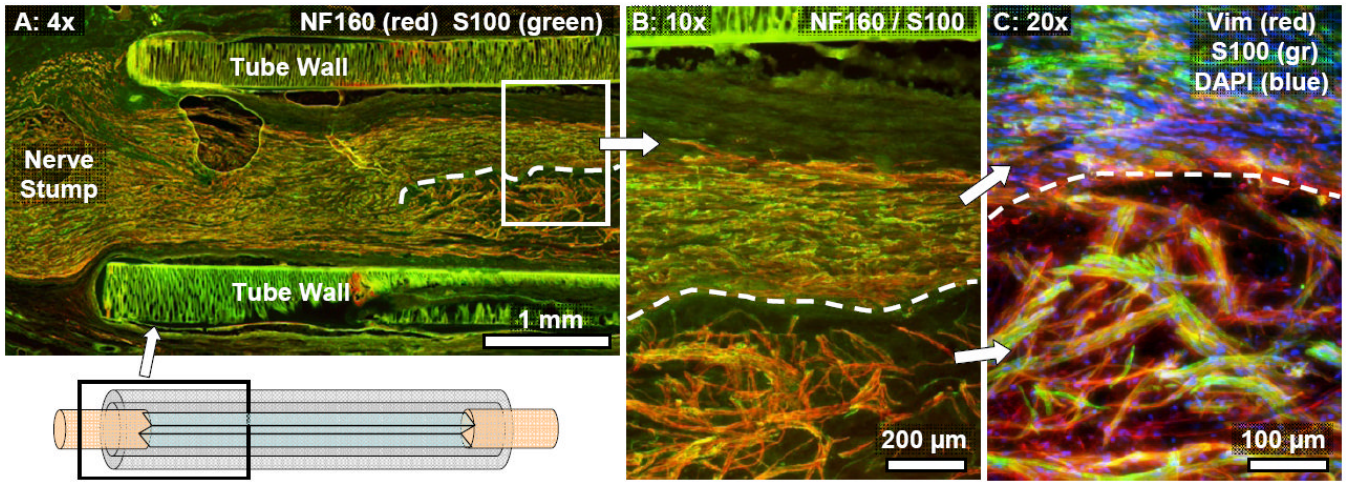

Fig. 10.

Longitudinal section from a 3-film channel at the six week time point. (A): Axons (NF160: red) and co-localized Schwann cells (S100: green) were regenerated into the different zones of the channel. The top outer thin-film is marked with a dashed line, and a diagram in the lower left corner illustrates the approximate location within the channel of the image. (B): Magnified view of the boxed region in (A). Regenerated axons and Schwann cells in the top outer zone (above the labeled thin-film) were longitudinally aligned, growing in a core that made direct contact with the aligned thin-film. Overlying peripheral bands of collagenous tissue were longitudinally aligned as well. In the interior zones underneath the top outer thin-film, regenerating axons and co-localized Schwann cells displayed disrupted patterns of longitudinal alignment. (C): Vimentin+ fibroblasts were randomly aligned in the inner zones.

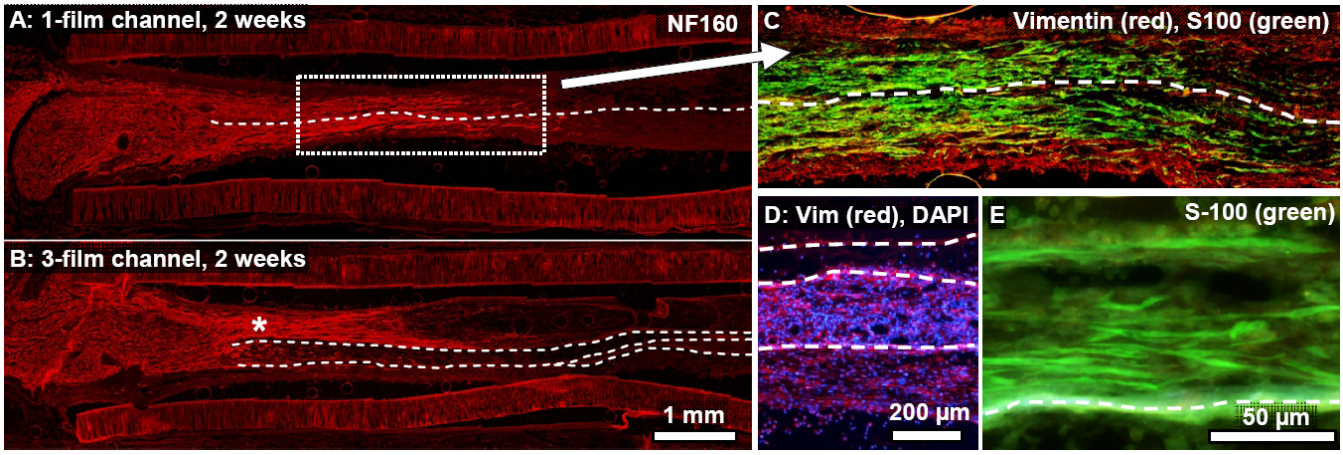

Fig. 11.

Longitudinal sections from a 1-film (A,C) and 3-film channel (B,D,E), two weeks post-surgery. (A,B): NF160+ axons had regenerated approximately one third of the distance through each channel type. Asymmetric growth of the regenerating axons into the topmost zone of this 3-film channel ('*' symbol) might have been due in part to the off-center location of the proximal nerve stump. Regeneration in the 1-film channel (A,C) was symmetrically distributed around the single thin film, although this was not always the case. (C): Magnified view of the boxed region in (A). Fibroblasts had fully bridged the gap. (D): Image from near the midpoint of the 3-film channels. Fibroblasts had fully bridged the gap and were distributed asymmetrically between the different zones of the 3-film channel (image taken near channel midpoint.) (E): Cross-section taken towards the distal end of the 3-film channel. Schwann cells, seen here migrating from the distal end, were highly aligned along the aligned thin-films, growing in direct contact with the thin-films, on top of each other, and also through the tissue matrix of the developing regeneration cable.

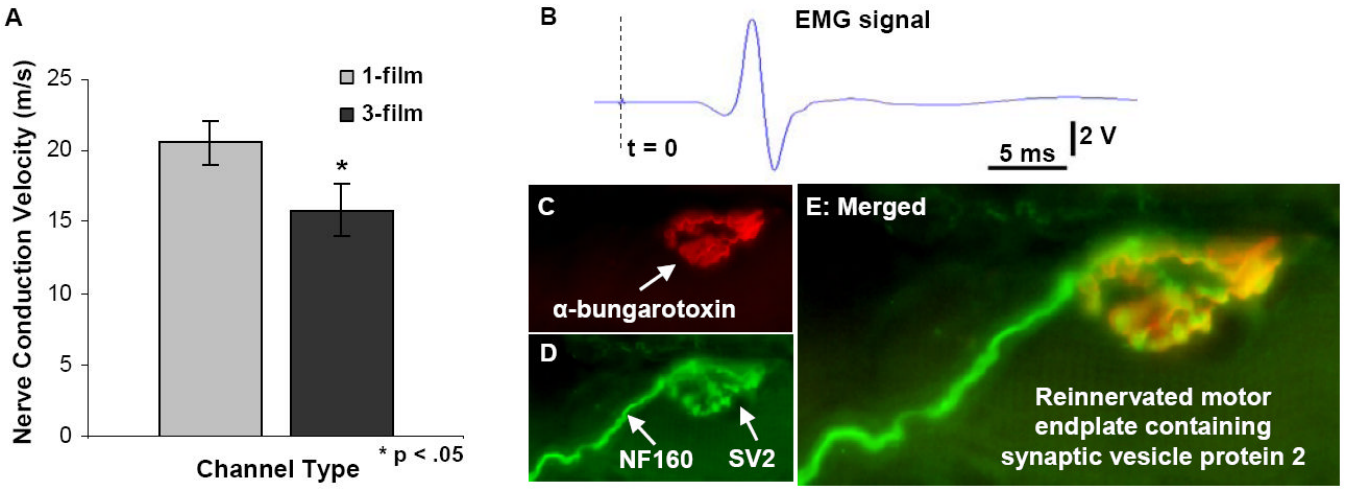

Fig. 12.

Evaluation of nerve conduction velocity and muscular reinnervation. (A): Significantly higher compound action potential conduction velocities were measured from nerves regenerated through the 1-film channels. (B): All gastrocnemius muscles produced measurable EMG signals and visible contractions. (This representative trace was taken from a 3-film channel case.) (C-E): As a further evaluation of muscular reinnervation, sectioned gastrocnemius muscles were reacted for immunofluorescent demonstration of (C) motor endplates, (D) axons, and vesicles containing synaptic vesicles 2 (SV2) protein. (E) Co-localization of these three markers confirmed the presence of reinnervated motor endplates in all treated animals.

Table 1

Experimental groups

Groups	No. of rats
1-film, 13 weeks	10
3-film, 13 weeks	10
1-film, 6 weeks	5
3-film, 6 weeks	5